ARTICLE OPEN

Check for updates

Phonon thermal transport shaped by strong spin-phonon scattering in a Kitaev material $Na_2Co_2TeO_6$

Xiaochen Hong[1,2]✉, Matthias Gillig[2], Weiliang Yao[3], Lukas Janssen[4]✉, Vilmos Kocsis[2], Sebastian Gass[2], Yuan Li[3,5], Anja U. B. Wolter[2], Bernd Büchner[2,6] and Christian Hess[1,2]✉

The report of a half-quantized thermal Hall effect and oscillatory structures in the magnetothermal conductivity in the Kitaev material α-$RuCl_3$ have sparked a strong debate on whether it is generated by Majorana fermion edge currents, spinon Fermi surface, or whether other more conventional mechanisms are at its origin. Here, we report low temperature thermal conductivity (κ) of another candidate Kitaev material, $Na_2Co_2TeO_6$. The application of a magnetic field (B) along different principal axes of the crystal reveals a strong directional-dependent **B** impact on κ, while no evidence for mobile quasiparticles except phonons can be concluded at any field. Instead, severely scattered phonon transport prevails across the $B-T$ phase diagram, revealing cascades of phase transitions for all **B** directions. Our results thus cast doubt on recent proposals for significant itinerant magnetic excitations in $Na_2Co_2TeO_6$, and emphasize the importance of discriminating true spin liquid transport properties from scattered phonons in candidate materials.

npj Quantum Materials (2024)9:18; https://doi.org/10.1038/s41535-024-00628-4

INTRODUCTION

Frustrated magnets refer to a set of materials that do not order down to temperatures well below the corresponding magnetic interaction strength. In some cases, the system is left with a ground state called quantum spin liquid (QSL), which is characterized by entangled spins, topological orders, and fractionalized magnetic excitations[1–3]. Kitaev QSL, proposed for bond-dependent nearest-neighbor interacting spins on the two-dimensional honeycomb lattice[4], is among the rare examples of exactly solvable QSL models[5–8]. Recent research interest is further fueled by possible achieving Kitaev QSL in realistic materials. In particular, fingerprints of QSL-related excitations were revealed in α-$RuCl_3$[9,10], both in its zero-field phase above the magnetic order[11], and more intriguingly, in its field-induced quantum disordered state[12].

However, those sought-after signatures for QSLs observed in α-$RuCl_3$ always come along with alternative explanations. To be more specific on transport experiments, the report of half-integer quantization of thermal Hall conductance was once regarded as a definitive proof for the existence of Majorana fermions in the field-induced quantum disordered state in α-$RuCl_3$[12]. However, following experiments noticed such quantization is less reproducible, and attributed the non-quantized temperature-dependent thermal Hall effect to phonons[13], or topological magnons[14]. On the other hand, quantum oscillations of longitudinal thermal conductivity in the quantum disordered state of α-$RuCl_3$ suggest some fractionalised magnetic excitations forming a Fermi surface[15]. But such spectacle is also argued to be a result simply due to scattered phonons[13,16], in particular taking into account that no itinerant magnetic excitation has been found in a previous low temperature work[17]. On top of all these inconsistencies are the facts that α-$RuCl_3$ suffers from the notorious stacking fault problem[18], from the dechlorination and oxidation after heat treatment[19], and more generally from sample dependence[20]. Thus, it is indispensable to seek for another example that can contribute to clarify to what extent these results are intrinsic to a Kitaev material.

In this paper, we studied the ground state properties of a quantum magnet $Na_2Co_2TeO_6$ (NCTO), which was recently investigated as a candidate Kitaev QSL[21–23], through the prism of low temperature thermal conductivity. Similar to its more famous cousin α-$RuCl_3$, NCTO also features an intermediate quantum disordered phase sandwiched between the low-field magnetically ordered state and the high-field polarized state[22,23], where a QSL state is prospected. In this work, we report an anisotropic and astonishing large **B** impact on κ at low temperatures (<1 K). The analysis of our data demonstrates that there is *no* evidence for mobile gapless QSL excitations (κ_{QSL}) contributing to κ. Instead, strongly scattered phonon transport (κ_{ph}), a quite traditional mechanism, is responsible for all the observed phenomena. Utilizing the high resolution $\kappa(B)$ data, we reveal a large density of magnetic excitations in the zero-field ground state of NCTO, further promoted excitations by magnetic field perpendicular to the honeycomb plane, and possible quantum criticality driven by in-plane magnetic field.

RESULTS AND DISCUSSION

$\kappa/T(T)$ in fixed magnet fields

The residual linear term of thermal conductivity extrapolated to the low temperature limit ($\kappa_0/T \equiv \kappa/T|_{T\to 0}$) is persistently scrutinized for QSL candidates[3,24], since its existence would suggest realization of some sought-after QSL states, including spinons forming a Fermi surface[25–29]. Figure 1a shows κ/T of five NCTO crystals in zero magnetic field as a function of T. Albeit certain

[1]Fakultät für Mathematik und Naturwissenschaften, Bergische Universität Wuppertal, 42097 Wuppertal, Germany. [2]Leibniz-Institute for Solid State and Materials Research (IFW-Dresden), 01069 Dresden, Germany. [3]International Center for Quantum Materials, School of Physics, Peking University, 100871 Beijing, China. [4]Institut für Theoretische Physik and Würzburg-Dresden Cluster of Excellence ct.qmat, Technische Universität Dresden, 01062 Dresden, Germany. [5]Collaborative Innovation Center of Quantum Matter, 100871 Beijing, China. [6]Institute of Solid State and Materials Physics and Würzburg-Dresden Cluster of Excellence ct.qmat, Technische Universität Dresden, 01062 Dresden, Germany. ✉email: xhong@uni-wuppertal.de; lukas.janssen@tu-dresden.de; c.hess@uni-wuppertal.de

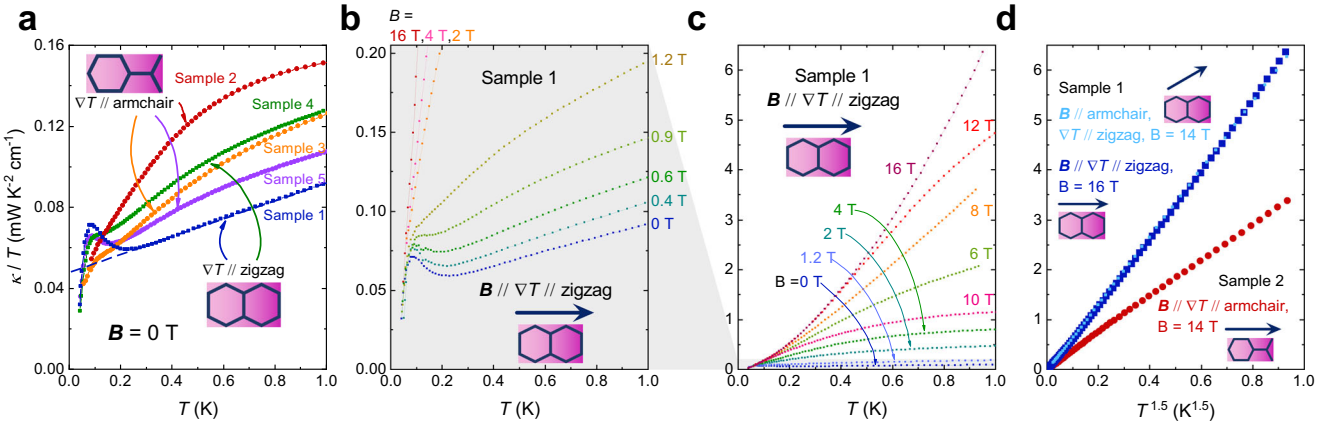

Fig. 1 Thermal conductivity of $Na_2Co_2TeO_6$ and the impact of the in-plane magnetic fields. a In-plane thermal conductivity of five $Na_2Co_2TeO_6$ crystals without magnetic field. The thermal gradient (∇T) was set || *zigzag* for Sample#1 and Sample#4, and || *armchair* for the other three samples. By extrapolating the data to $T = 0$ K, a residual linear term ($\kappa/T|_{T\to 0}$) can be resolved for all five $\kappa/T(T)$ curves, especially clear for Sample#1, as indicated by the dashed blue line. **b** The field dependence of the $\kappa/T(T)$ curves for Sample#1, focusing on the small field limit which covers a small portion of (**c**), the full field dependence of the $\kappa/T(T)$ curves, as indicated by the gray background. At $T = 1$ K, the κ of Sample#1 experience a 70-fold increase from $B = 0$ T to the saturation field. **d** The $\kappa/T(T)$ curves display a typical phononic $\propto T^{\alpha}$ behavior with $\alpha = 1.5$ at high enough fields. The field direction does not affect the saturated $\kappa/T(T)$ curves.

sample dependence, the $\kappa/T(T)$ profiles of all investigated crystals do not follow the simple power-law behavior expected for common insulators. Instead, regardless of the direction along which the thermal gradient ∇T is established (the two in-plane principal axes for the Co-honeycomb lattice, denoted as *zigzag* and *armchair* directions, indicated by the schematic insets), all $\kappa/T(T)$ profiles trend to end with a finite κ_0/T.

Among them, Sample#1 is especially notable for displaying a pronounced hump which emerges below about 250 mK. κ_0/T of Sample#1, extracted from a linear fit to its data above 250 mK, as highlighted by the dashed line in Fig. 1a, is 0.048 $mW/K^{-2}\,cm^{-1}$. At first glance, this finite κ_0/T is consistent with the notion that the ground state of NCTO is a QSL, since κ_{QSL} contributed by a putative spinon Fermi surface is expected to scale linearly with T at the lowest temperatures[24]. We are aware of a recent work reporting similar data of NCTO, where these results have been interpreted as evidences for κ_{QSL}[30]. However, as clearly shown in Fig. 1a, the upturn of $\kappa/T(T)$ for Sample#1 (same for Sample#4 and Sample#5) terminates abruptly below about 100 mK, followed by a sharp drop, which results in a vanishing residual linear term that is incompatible with a gapless QSL ground state. Furthermore, we argue such observation is at odds with a hypothesised gapped QSL state with a gap size of the orderb~100 mK. When a small in-plane magnetic field is applied, $\kappa_{QSL}/T(T)$ at temperatures below the initial gap energy scale is expected to increase due to a proliferation of quasiparticle excitations, while $\kappa/T(T)$ at higher temperatures should be less sensitive to the field since κ_{ph} is not directly affected. This is just opposite to our observations. As depicted in Fig. 1b, the field changes $\kappa/T(T)$ fundamentally above 100 mK, while it has basically no impact on the data at the lowest temperature.

Higher magnetic fields have a drastic impact on the $\kappa(T)/T$ curves until they finally saturate into a power-law behavior over the whole temperature range at the highest field. A representative case of Sample#1 is shown in Fig. 1c, along with the others displayed in Supplementary Note 1. As can be seen in Fig. 1d, regardless of the (in-plane) field directions, $\kappa(T)/T$ curves for a given sample saturate at the same value.

Recent high-field magnetization experiments found the field-polarized state is reached for in-plane magnetic field higher than 10 T in NCTO[31]. As a result, spins are expected to neither contribute directly, nor indirectly through scattering phonons though pertinent fluctuations at the highest field reached in this study. The saturated $\kappa(T)/T$ thus represents a background phonon heat conductivity κ_{ph} in the low-temperature limit with $\kappa_{ph}/T \propto T^{\alpha}$, of which the exponent $\alpha = 1.5$. For ballistic phonons condition, usually reached at the low temperature region, $\alpha = 2$ should be expected, unless the phonon reflection at the sample surface is not perfectly diffuse. As discussed in Supplementary Note 1, there is no sign of phonon men free path exceeding boundaries scattering limit. Thus a more likely explanation of the the deviation from the $\alpha = 2$ expectation could be attributed ti non-magnetic and/or non-point-like disorders (spatially extended to mm-length that is comparable to phonon wavelength at low temperature) inside the sample. Obviously, the highest field applied in this work is insufficient to affect on this scattering. Thus, the $\kappa(T)/T$ curves at highest in-plane field are token as the phonon thermal conductivity $\kappa_{ph}/T(T)$ free scattering off magnetic fluctuations. We are aware that $\alpha < 2$ is quite common among frustrated magnet systems[17,32,33], and $\alpha \approx 1.5$ is especially frequently observed.

As can be concluded from Fig. 1 and Supplementary Figure 1, there is no evidence for finite κ_0/T at any field. Furthermore, $\kappa/T(T)$ profiles at zero and low fields never exceed the saturated $\kappa_{ph}/T(T)$ over the whole temperature range. Hence, any evidence for a direct magnetic thermal transport channel on top of κ_{ph}, including κ_{QSL}, is elusive. If present, it must be negligibly small since the total measured κ at zero field is already at a very small value and at finite fields the saturated κ_{ph} is never exceeded. Hence, the intricate landscape of $\kappa(T)/T$ and its field dependence can be reasonably accounted for by strong phonon-spin scattering, which is the main theme of the rest of the paper. We wish to mention that the above-mentioned zero-field low-temperature hump of $\kappa(T)/T$ can be a result of scattered phonon transport, but some direct magnetic thermal transport contributions can not be excluded from our results.

In-plane magnetic field dependence of κ/T at fixed temperature

The field dependence of $\kappa/T(T)$ is non-monotonic, see Fig. 1c. A closer inspection can be performed by isothermal $\kappa/T(B)$ measurements. Figure 2a–c exhibits the representative data of two samples with three different (∇T, **B**) direction combinations. A straightforward conclusion is that $\kappa(B)$ is dictated by the **B** direction, irrelevant to the ∇T direction. That further underlines the dominance of scattered κ_{ph} in NCTO over the whole field-

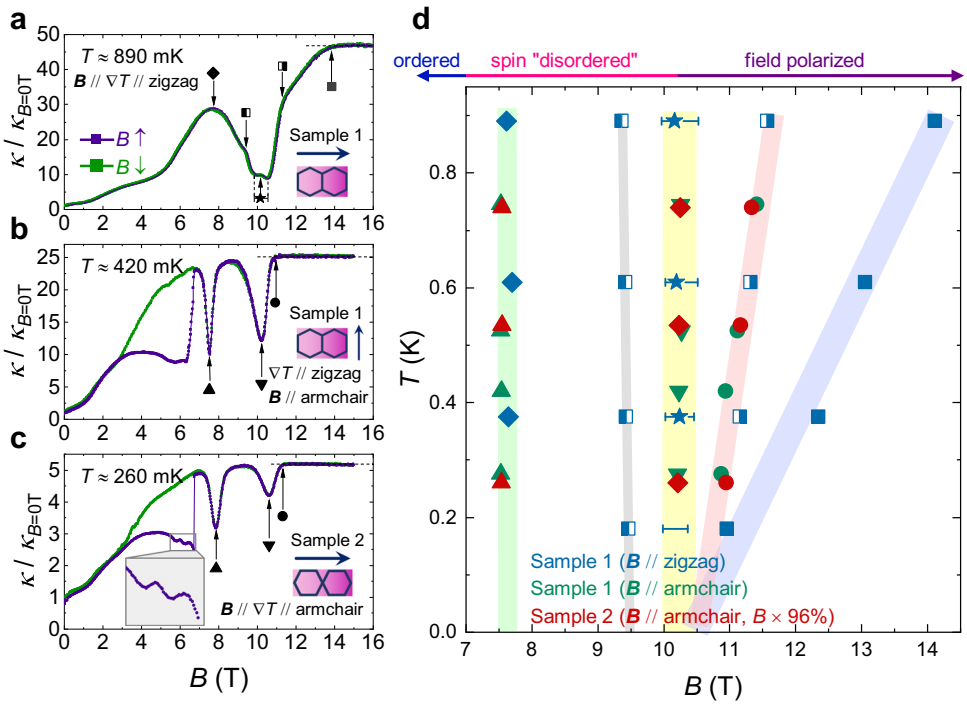

Fig. 2 Anisotropic in-plane magnetic field effects on the thermal conductivity. Panels **a**–**c**, plot the normalized $\kappa(B)$ profiles of different combinations of (∇T, B) orientations at selected temperatures. The purple curves and the green curves depict the data collected with field increasing and decreasing, respectively. All $\kappa(B)$ curves experience a saturation at high fields, signaling that a polarized state was reached in this study. Panels **a** and **b** depict the results of the same crystal (Sample#1) with the same ∇T orientation ($\nabla T \parallel$ *zigzag*) but with different **B** directions. They behave fundamentally different. Meanwhile, Panel **b** resembles Panel **c** which is the data collected from another crystal (Sample#2) with a different ∇T orientation ($\nabla T \parallel$ *armchair*) but the same field direction (**B** || *armchair*). As highlighted in the inset of Panel **c**, an oscillation-like feature can be distinguished before an abrupt increase of the $\kappa(B)$ for the field-up ramp. The anomalies in all $\kappa/T(B)$ curves are marked by different symbols. **d** The temperature evolution of these anomalies of $\kappa(B)$ profiles in the "spin disordered" state and field polarized state, as indicated by the colored arrow above the panel. They are grouped into different categories as glided by the background stripes. The field values for Sample#2 are multiplied by 96%, in order to compromise the possible (out-of-plane) misalignment.

temperature phase space. More specifically, a magnetic field applied along the *zigzag* and *armchair* directions on the same sample results in sharply different $\kappa(B)$ profiles. For **B** || *zigzag* (Fig. 2a), there is strictly *no* hysteresis behavior. The overall feature turns out to be a broad dip centered around 10.2 T, with many minor anomalies marked by different symbols in the figure. For **B** || *armchair* (Fig. 2b, c and Supplementary Figure 2e–k), there are two very sharp dips at 7.5 T and 10.2 T. In contrast to the **B** || *zigzag* case, a large hysteresis between 3 T and 6.5 T is evident. The abrupt increase of κ in the up-ramp isotherm points to a first-order-like transition. Note that the **B** direction-dependent occurrence of hysteresis was already mentioned by higher temperature investigations[23,34]. More discussion on the hysteretic behavior can be found in the Supplementary Note 2. With both **B** directions, κ saturates at high enough fields, as indicated by the dashed lines.

All the salient features in Fig. 2a–c and Supplementary Figure 2 are summarized in Fig. 2d. Beside the saturation field, which increases roughy linearly with temperature, the other anomalies are basically temperature independent. Such rich phase diagram suggests the landscape of successive **B** induced phase transitions of the Heisenberg-Kitaev model might be inherited by NCTO[35]. Remarkably, three different finite-temperature anomalies marked by the yellow, red, and blue shaded areas seem to merge at around 10.2 T at 0 K, suggesting a quantum critical point. We expect the presented result to motivate further theoretical studies that account for specified parameters of NCTO in order to demystify these phases.

Some theoretical exploration on the Heisenberg-Kitaev honeycomb model have already revealed the potentially very rich phase diagram tuned by magnetic field[35]. Of particular interest is a multi-Q phase that can be stabilized in finite fields[35]. Recent experiments proposed the zero-field ground state of NCTO could be a triple-Q order[36–40], potentially stabilized by the proposed ring exchange interactions[38]. If confirmed, it could be a natural explanation of the extensive scattering of κ_{ph} at zero field, since a triple-Q ordered state guarantees larger density of state (DOS) of excitations around zero momentum (Γ point) which interact strongly with phonons[38]. These magnetic excitations should in principle contribute to specific heat. A decent experiment to exam this property is still pending for NCTO since heat capacity measurement at very low temperature is technically challenging[41]. Nevertheless, in Supplementary Note 3 we argue our raw data can provide some indirect evidences for huge specific heat in the zero-field ground state. Our data thus corroborate the notion of very large magnetic DOS as is expected for a triple-Q state.

Next we comment on the oscillation-like $\kappa(B)$ in the intermediate field range when **B** || *armchair*, as highlighted in the inset of Fig. 2c. A similar feature exists but is less obvious in another sample and at higher temperatures, see Supplementary Figure 2g, h, and j. Gapless QSL states that foster quantum oscillation of presumably charge neutral magnetic excitations are indeed anticipated for the Kitaev model[4,42,43], and was invoked to interpret the $\kappa(B)$ oscillations in α-$RuCl_3$[15]. Nevertheless, we believe quantum oscillations of κ_{QSL} should be irrelevant to NCTO. First of all, the oscillation feature in NCTO exists in the hysteresis region, thus in a magnetically ordered state. Besides, the fact that there is no evidence for itinerant κ_{QSL} at any field does not favor a quantum oscillation picture. Additionally, it is hard to imagine a significant direct contribution of κ_{QSL} which is exempted from the

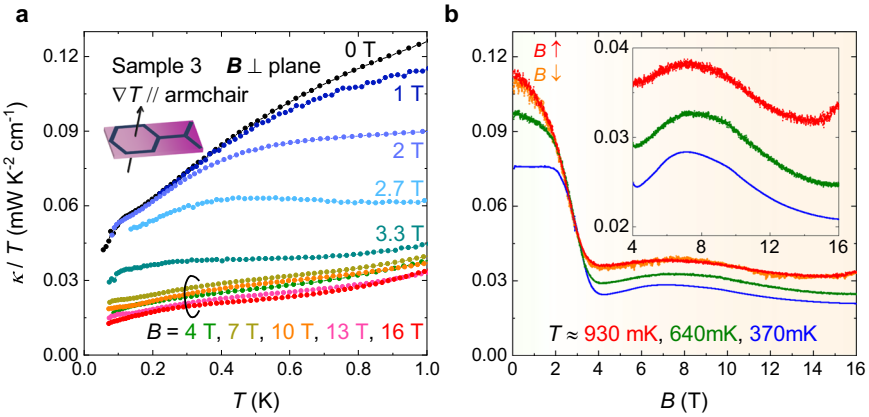

Fig. 3 Further suppression of κ by out-of-plane magnetic fields. a The in-plane κ of Sample#3 under out-of-plane magnetic fields. The geometry is sketched in the inset. ∇T is along the *armchair* direction, and **B** is perpendicular to the honeycomb plane. A rapid field suppression of κ/T is recognized at finite temperatures below about 3 T. At higher fields, the $\kappa/T(T)$ curves changes nonmonotonically in a narrow range. **b** The $\kappa/T(B)$ profiles at three representative temperatures. They clearly show a fast drop at field $2\ T < B < 4\ T$, followed by an oscillation-like feature at higher fields. As highlighted in the inset, the oscillation profiles change little with temperature.

strong fluctuations that results in a reduction of κ_{ph} by orders of magnitude. With this in mind, more caution should be taken for uniqueness of possible Kitaev QSL signatures observed in this material class, since thermal transport properties of NCTO share impressively similar features with α-$RuCl_3$[23,44–46]. Indeed, a recent careful investigation on the oscillatory structures of $\kappa(B)$ of α-$RuCl_3$ indeed addressed all the dips to certain magnetic phase transitions[16]. We stress that our observation in a similar but simpler sample system further supports this conclusion.

Out-of-plane magnetic field impact on κ

Finally, at low temperatures, when **B** is applied perpendicular to the NCTO honeycomb plane, κ gets further suppressed beyond a critical field of $B \approx 3$ T, as shown in Fig. 3a. In the language of magnetic scattering, it means the already strong magnetic fluctuations at zero field are even further promoted, contradictory to the intuition that field alignment of the magnetic moments should reduce them.

Indeed, there are some theoretical considerations predicting $\mathbf{B} \parallel c$ can lead to abundant phase transitions in the original Kitaev model and its variants[35,42,47–49]. Especially, quantum fluctuations in some of these intermediate phases are expected to be rather strong[49], in line with our observations that κ_{ph} gets further suppressed compared to the zero-field phase. As displayed more clearly in Fig. 3b, $\kappa/T(B)$ experiences a rapid drop between 2 T and 4 T. It is non-monotonic at higher field, featured by a broad hump around 8 T and a broad dip around 15 T, highlighted by the inset. We note the anomaly at about 15 T can be related to phase transitions revealed by a recent magnetization work[31], while the rapid drop between 2 T and 4 T do not have a similar correspondence.

To conclude, our high-quality low-temperature thermal transport study on NCTO single crystals established the dominance of phonon thermal transport in its magnetic ground states, and exclude a significant direction contribution from itinerant magnetic excitations (Please be aware magnon excitation contribution to the transverse thermal transport was detected[46]). The field evolution of κ, which manifests the strength of phonon-spin scattering, was taken as a probe to elucidate the intricate magnetic phases in NCTO. The strongly scattered phonons in the zero-field ground state indicate large DOS of magnetic excitations, in line with the proposal of a triple-Q state in NCTO. The in-plane κ depends significantly of the in-plane field direction, underlines the bond-dependent interactions of a Kitaev material. However, a criticality at 10.2 T is present regardless of the in-plane field direction. Field perpendicular to the honeycomb plane also induces multiple magnetic phases, where phonon-spin scattering is even more prominent than the zero-field phase. We expect similar physics should be quite common among QSL candidate materials, since QSLs are intrinsically at the edge of competing orders. The pervasive phase boundaries should be careful considered when analyzing existing and future experimental results of QSL candidate materials.

METHODS

Sample preparation

Single crystals of $Na_2Co_2TeO_6$ were prepared with a modified flux method. Na_2CO_3, Co_3O_4, and TeO_2 powders were grounded and loaded into an alumina crucible. Excess amount of TeO_2 served as a self-flux. The crucible was heated up to 1050 °C, kept for two days, before cooling down to 600 °C at a rate of 6.5 °C per hour. Ruby-colored hexagonal flakes of typical size $\sim 10 \times 10 \times 0.1$ mm^3 can be mechanically collected out of bluish violet residue. The harvested single crystals were further washed with a NaOH solution. Basic characterizations of the as-grown crystals can be found in ref. [34].

The samples were cut into a size of about $\sim 5 \times 1 \times 0.1$ mm^3, the longest direction along which ∇T was generated are the *armchair* or *zigzag* directions, respectively. In order to make thermal contacts to the fresh surface, the out-most layers of the as-grown crystals were cleaved off by a blade just before the silver paint was glued to it. As a result, the thickness of the samples were reduced to about 60 μm.

Heat transport measurements

The thermal conductivities were measured in a dilution refrigerator, using a standard four-wire steady-state method with two RuO_2 chip thermometers, calibrated in situ against a reference RuO_2 thermometer. For fixed field $\kappa(T)$ measurements, each sample was initially cooled down from room temperature without magnetic field. The data were collected with gradually increased magnetic field in order to avoid the complicated situation of involving the hysteresis effect. $\kappa(T)$ data were collected in a steady-state manner (see Supplementary Figure 3).

To measure the $\kappa(B)$ isotherms, the system was cooled from the paramagnetic phase in zero field. Then the sample temperature was kept at a set point, and the field was changed from 0 T to the highest field (up-ramp), followed by decreasing to 0 T (down-ramp). The field was changed at a speed no more than 20 mT per minute, in order to

minimize its heating effect, and to keep the system in a (quasi-) thermal equilibrium state. In some cases, the field were ramped up and down multiple times, see Supplementary Note 2 for more details.

We wish to point out that according to our experience, NCTO seems to have very strong anisotropic in-plane magnetic susceptibility at very low temperatures, that tend to align the *armchair* direction to the field. We are aware of a recently posted paper which reports a direct measurement of this magnetic anisotropy that underpins our conjecture[50]. In order to avoid experimental artifacts caused by such effect, the cooler side of all samples were glued to the heat sink (a gilded silver bulk) directly with a strong epoxy (Wakefield DeltaBond-152 two component adhesives). The samples and the wires attached to them were checked carefully under a microscope after the experiments, to confirm they had not bent during the measurements.

Thermodynamic measurements

The magnetization measurements were carried out using a SQUID magnetometer (iHelium3, MPMS-XL, Quantum Design). The magnetostriction was measured using a commercially available dilatometer (Standard probe, Kuechler) compatible with the Quantum Design PPMS systems. These measurements are based on the capacitance measurement technique (AH2700A, Andeen-Hagerling).

DATA AVAILABILITY

The data that support the findings of this study are available from the corresponding authors upon reasonable request.

Received: 17 July 2023; Accepted: 19 January 2024;
Published online: 10 February 2024

REFERENCES

1. Balents, L. Spin liquids in frustrated magnets. *Nature* **464**, 199–208 (2010).
2. Savary, L. & Balents, L. Quantum spin liquids: a review. *Rep. Prog. Phys.* **80**, 106502 (2017).
3. Zhou, Y., Kanoda, K. & Ng, T. K. Quantum spin liquid states. *Rev. Mod. Phys.* **89**, 025003 (2017).
4. Kitaev, A. Anyons in an exactly solved model and beyond. *Ann. Phys.* **321**, 2–111 (2006).
5. Moessner, R. & Sondhi, S. L. Resonating valence bond phase in the triangular lattice quantum dimer model. *Phys. Rev. Lett.* **86**, 1881 (2001).
6. Wen, X.-G. Quantum orders in an exact soluble model. *Phys. Rev. Lett.* **90**, 016803 (2003).
7. Yao, H., Zhang, S.-C. & Kivelson, S. A. Algebraic spin liquid in an exactly solvable spin model. *Phys. Rev. Lett.* **102**, 217202 (2009).
8. Ben-Zion, D., Das, D. & McGreevy, J. Exactly solvable models of spin liquids with spinons, and of three-dimensional topological paramagnets. *Phys. Rev. B* **93**, 155147 (2016).
9. Takagi, H., Takayama, T., Jackeli, G., Khaliullin, G. & Nagler, S. E. Concept and realization of Kitaev quantum spin liquids. *Nat. Rev. Phys.* **1**, 264–280 (2019).
10. Broholm, C. et al. Quantum spin liquids. *Science* **367**, 263 (2020).
11. Banerjee, A. et al. Proximate Kitaev quantum spin liquid behavior in a honeycomb magnet. *Nat. Mat.* **15**, 733–740 (2016).
12. Kasahara, Y. et al. Majorana quantization and half-integer thermal quantum Hall effect in a Kitaev spin liquid. *Nature* **559**, 227–231 (2018).
13. Lefrançois, É. et al. Oscillations in the magnetothermal conductivity of α-$RuCl_3$: evidence of transition anomalies. *Phys. Rev. B* **107**, 064408 (2023).
14. Czajka, P. et al. Planar thermal Hall effect of topological bosons in the Kitaev magnet α-$RuCl_3$. *Nat. Mater.* **22**, 36–41 (2023).
15. Czajka, P. et al. Oscillations of the thermal conductivity in the spin-liquid state of α-$RuCl_3$. *Nat. Phys.* **17**, 915–919 (2021).
16. Bruin, J. A. N. et al. Origin of oscillatory structures in the magnetothermal conductivity of the putative Kitaev magnet α-$RuCl_3$. *APL Mater.* **10**, 090703 (2022).
17. Yu, Y. J. et al. Ultralow-temperature thermal conductivity of the Kitaev honeycomb magnet α-$RuCl_3$ across the field-induced phase transition. *Phys. Rev. Lett.* **120**, 067202 (2018).
18. Zhang, H. et al. Stacking disorder and thermal transport properties of α-$RuCl_3$. *Phys. Rev. Materials* **8**, 014402 (2024).
19. Breitner, F. A., Jesche, A., Tsurkan, A. & Gegenwart, P. Thermal decomposition of the Kitaev material α-$RuCl_3$ and its influence on low-temperature behavior. *Phys. Rev. B* **108**, 045103 (2023).
20. Kasahara, Y. et al. Quantized and unquantized thermal Hall conductance of the Kitaev spin liquid candidate α-$RuCl_3$. *Phys. Rev. B* **106**, L060410 (2022).
21. Liu, H. & Khaliullin, G. Pseudospin exchange interactions in d^7 cobalt compounds: possible realization of the Kitaev model. *Phys. Rev. B* **97**, 014407 (2018).
22. Lin, G. et al. Field-induced quantum spin disordered state in spin-1/2 honeycomb magnet $Na_2Co_2TeO_6$. *Nat. Commun.* **12**, 5559 (2021).
23. Hong, X. et al. Strongly scattered phonon heat transport of the candidate Kitaev material $Na_2Co_2TeO_6$. *Phys. Rev. B* **104**, 144426 (2021).
24. Yamashita, M., Shibauchi, T. & Matsuda, Y. Thermal-transport studies on two-dimensional quantum spin liquids. *Chemphyschem* **13**, 74–78 (2012).
25. Yamashita, M. et al. Highly mobile gapless excitations in a two-dimensional candidate quantum spin liquid. *Science* **328**, 1246–1248 (2010).
26. Hartstein, M. et al. Fermi surface in the absence of a Fermi liquid in the Kondo insulator SmB_6. *Nat. Phys.* **14**, 166–172 (2018).
27. Li, N. et al. Possible itinerant excitations and quantum spin state transitions in the effective spin-1/2 triangular-lattice antiferromagnet $Na_2BaCo(PO_4)_2$. *Nat. Commun.* **11**, 4216 (2020).
28. Sato, Y. et al. Charge-neutral fermions and magnetic field-driven instability in insulating $YbIr_3Si_7$. *Nat. Commun.* **13**, 394 (2022).
29. Pan, B. et al. Unambiguous experimental verification of linear-in-temperature spinon thermal conductivity in an antiferromagnetic Heisenberg chain. *Phys. Rev. Lett.* **129**, 167201 (2022).
30. Guang, S. K. et al. Thermal transport of fractionalized antiferromagnetic and field-induced states in the Kitaev material $Na_2Co_2TeO_6$. *Phys. Rev. B* **107**, 184423 (2023).
31. Zhang, S. et al. Electronic and magnetic phase diagrams of the Kitaev quantum spin liquid candidate $Na_2Co_2TeO_6$. *Phys. Rev. B* **108**, 064421 (2023).
32. Barthélemy, Q. et al. Heat conduction in herbertsmithite: field dependence at the onset of the quantum spin liquid regime. *Phys. Rev. B* **107**, 054434 (2023).
33. Fauqué, B. et al. Thermal conductivity across the metal-insulator transition in the single-crystalline hyperkagome antiferromagnet $Na_{3+x}Ir_3O_8$. *Phys. Rev. B* **91**, 075129 (2015).
34. Yao, W. & Li, Y. Ferrimagnetism and anisotropic phase tunability by magnetic fields in $Na_2Co_2TeO_6$. *Phys. Rev. B* **101**, 085120 (2020).
35. Janssen, L., Andrade, E. C. & Vojta, M. Honeycomb-lattice Heisenberg-Kitaev model in a magnetic field: spin canting, metamagnetism, and vortex crystals. *Phys. Rev. Lett.* **117**, 277202 (2016).
36. Chen, W. et al. Spin-orbit phase behavior of $Na_2Co_2TeO_6$ at low temperatures. *Phys. Rev. B* **103**, L180404 (2021).
37. Lee, C. H. et al. Multistage development of anisotropic magnetic correlations in the Co-based honeycomb lattice $Na_2Co_2TeO_6$. *Phys. Rev. B* **103**, 214447 (2021).
38. Krüger, W. G. F., Chen, W., Jin, X., Li, Y. & Janssen, L. Triple-Q order in $Na_2Co_2TeO_6$ from proximity to hidden-SU(2)-symmetric point. *Phys. Rev. Lett.* **131**, 146702 (2023).
39. Yao, W. et al. Magnetic ground state of the Kitaev $Na_2Co_2TeO_6$ spin liquid candidate. *Phys. Rev. Research* **5**, L022045 (2023).
40. Kikuchi, J. et al. Field evolution of magnetic phases and spin dynamics in the honeycomb lattice magnet $Na_2Co_2TeO_6$: ^{23}Na NMR study. *Phys. Rev. B* **106**, 224416 (2022).
41. Wilhelm, H., Lühmann, T., Rus, T. & Steglich, F. A compensated heat-pulse calorimeter for low temperatures. *Rev. Sci. Instrum.* **75**, 2700–270 (2004).
42. Gohlke, M., Moessner, R. & Pollmann, F. Dynamical and topological properties of the Kitaev model in a [111] magnetic field. *Phys. Rev. B* **98**, 014418 (2018).
43. Hickey, C. & Trebst, S. Emergence of a field-driven U(1) spin liquid in the Kitaev honeycomb model. *Nat. Commun.* **10**, 530 (2019).
44. Hentrich, R. et al. Unusual phonon heat transport in α-$RuCl_3$: strong spin-phonon scattering and field-induced spin gap. *Phys. Rev. Lett.* **120**, 117204 (2018).
45. Hentrich, R. et al. Large thermal Hall effect in α-$RuCl_3$: evidence for heat transport by Kitaev-Heisenberg paramagnons. *Phys. Rev. B* **99**, 085136 (2019).
46. Gillig, M. et al. Phononic-magnetic dichotomy of the thermal Hall effect in the Kitaev material $Na_2Co_2TeO_6$. *Phys. Rev. Res.* **5**, 043110 (2023).
47. Sørensen, E. S., Catuneanu, A., Gordon, J. S. & Kee, H.-Y. Heart of entanglement: chiral, nematic, and incommensurate phases in the Kitaev-Gamma ladder in a field. *Phys. Rev. X* **11**, 011013 (2021).
48. Li, H. et al. Identification of magnetic interactions and high-field quantum spin liquid in α-$RuCl_3$. *Nat. Commun.* **12**, 4007 (2021).
49. Chern, L. E., Kaneko, R., Lee, H.-Y. & Kim, Y. B. Magnetic field induced competing phases in spin-orbital entangled Kitaev magnets. *Phys. Rev. Research* **2**, 013014 (2020).
50. Lin, G. et al. Evidence for field induced quantum spin liquid behavior in a spin-1/2 honeycomb magnet. Preprint at https://doi.org/10.21203/rs.3.rs-2034295/v1 (2022).

ACKNOWLEDGEMENTS

We thank Jeroen van den Brink, Matthias Vojta, Vladislav Kataev, Christoph Wellm, Satoshi Nishimoto, Wenjie Chen, Yang Xu, and Wilhelm Krüger for illuminating discussions and

collaboration on related work. We would like to thank Nicolás Pérez for generously sharing the equipment, and thank Danny Baumann and Tino Schreiner for their technical assistance, especially during the pandemic lab-shutdown crisis. This work has been supported by the Deutsche Forschungsgemeinschaft (DFG) through SFB 1143 (Project-ID No.247310070) and the Würzburg-Dresden Cluster of Excellence *ct. qmat* (EXC 2147, Project-ID No. 390858490). C.H. has received funding from the European Research Council (ERC) under the European Union's-Horizon 2020 research and innovation program (Grant Agreement No. 647276-MARS-ERC-2014-CoG). L.J. was supported by the DFG through the Emmy Noether program (JA2306/4-1, Project No. 411750675). V.K. was supported by the Alexander von Humboldt Foundation. Y.L. acknowledges funding support from the National Basic Research Program of China (Grant No. 2021YFA1401901) and the NSF of China (Grant No. 12061131004).

AUTHOR CONTRIBUTIONS

B.B., C.H., and Y.L. conceived and initiated the study. W.Y. and Y.L. grown the crystals. X.H. and M.G. performed the transport measurements. V.K., S.G., and A.U.B.W. performed the thermodynamic measurements. X.H., C.H., and L.J. analyzed the data. X.H., C.H., L.J., and V.K. wrote the manuscript with input from all authors. C.H. supervised the project.

FUNDING

Open Access funding enabled and organized by Projekt DEAL.

COMPETING INTERESTS

The authors declare no competing interests.

ADDITIONAL INFORMATION

Supplementary information The online version contains supplementary material available at https://doi.org/10.1038/s41535-024-00628-4.

Correspondence and requests for materials should be addressed to Xiaochen Hong, Lukas Janssen or Christian Hess.